

Ex-situ Variable Angle Spectroscopic Ellipsometry of Iron Oxide Thin Films

Saira Riaz¹⁾, Hassan Yousaf²⁾, Shumaila Islam³⁾, *Zohra N. Kayani⁴⁾
and Shahzad Naseem⁵⁾

^{1), 2), 5)} *Centre of Excellence in Solid State Physics, University of Punjab, Lahore, Pakistan*

³⁾ *Laser Centre, University Technology, Malaysia*

⁴⁾ *Department of Physics, LCWU, Lahore, Pakistan*

⁵⁾ shahzad.cssp@pu.edu.pk

ABSTRACT

With the commercialization of spectroscopic ellipsometry instruments in the mid-1990s, the ellipsometry technique became quite popular, and now is applied to wide research areas from semiconductors to organic materials. Recent developments in spectroscopic ellipsometry have further allowed the real-time characterization of film growth and evaluation of optical anisotropy. Consequently, spectroscopic ellipsometry has established its position as a high precision optical characterization technique. Ellipsometry is an optical measurement technique that characterizes light reflection (or transmission) from samples. The key feature of ellipsometry is that it measures the change in polarized light upon light reflection on a sample. Iron oxide thin films are prepared using cost effective and low temperature sol-gel method. Four films are prepared with variation in pH of sol as 1, 2, 3 and 4. Optical properties of iron oxide thin films are studied using M-2000 Variable Angle Spectroscopic Ellipsometer. Films show high transmission in the visible and infrared region. Band gap of the films lies in the range of 2.15-2.17eV. Cauchy model is used to fit the experimental data for obtaining desired optical properties including refractive index and extinction coefficient. Decrease in refractive index and extinction coefficient is observed with increase in wavelength indicative of normal dispersion behavior.

1. INTRODUCTION

In field of science and technology, iron oxide is of particular importance. Almost 15 different phases of iron oxide and hydroxide are known to exist. It is not only used as electrode in lithium ion batteries and spintronic devices but also in diverse fields like optical computing. It offers the advantages of high optical susceptibility in non-linear optics (Ali et al. 2015, Aragon et al. 2016).

In the middle of different polymorphs three important stoichiometric types are Magnetite (Fe_3O_4), Maghemite ($\gamma\text{-Fe}_2\text{O}_3$) and Hematite ($\alpha\text{-Fe}_2\text{O}_3$). Magnetite (Fe_3O_4 or $\text{FeO}\cdot\text{Fe}_2\text{O}_3$) have inverse spinel cubic structure. Oxygen ions are positioned in cubic

close packed arrangement. Fe^{2+} (ferrous) cations are present on the octahedral sites. Fe^{3+} (ferric) cations are present on the octahedral and tetrahedral site. Maghemite ($\gamma\text{-Fe}_2\text{O}_3$) is the transition phase between Fe_3O_4 and hematite $\alpha\text{-Fe}_2\text{O}_3$. It also has cubic inverse spinel crystal structure similar to that of Fe_3O_4 . But in this case the sublattice is vacant due to absence of Fe^{2+} cations (Kulkarni and Lokhande 2003). Hematite ($\alpha\text{-Fe}_2\text{O}_3$) has hexagonal corundum arrangement. Oxygen anions are arranged in hexagonal close pack (hcp) frame work. Fe(III) cations are arranged on octahedral sites. Magnetite and maghemite are both ferrimagnetic at room temperature and show superparamagnetic behavior below a critical size limit (Riaz et al. 2014a,b, Akbar et al. 2014a,b, Akbar et al. 2015). At room temperature, hematite $\alpha\text{-Fe}_2\text{O}_3$ is weakly ferromagnetic below Curie temperature of 956K (683°C). Magnetite is the only polymorph of iron oxide that is a conductor at room temperature and its conductivity is because of the electron hopping process between ferrous (Fe^{+2}) and ferric (Fe^{+3}) ions and magnetite is the only phase that is half metallic at room temperature with spin polarization of 100% (Betram et al. 2012, Teja et al. 2009).

In this work crystalline $\alpha\text{-Fe}_2\text{O}_3$ thin films are deposited onto glass substrates. Iron oxide sols were synthesized with variation in pH value. The role of pH on optical properties (absorption coefficient, the band-gap, optical constants and dielectric constant) of the iron oxide thin films has been studied.

2. EXPERIMENTAL DETAILS

Preparation of iron oxide thin films was done using sol-gel and spin coating method. Starting material used was $\text{Fe}(\text{NO}_3)_3 \cdot 9\text{H}_2\text{O}$. It was mixed in solvents (water and ethylene glycol) to obtain solution. The solution was heated 80°C to obtain sol. Details of sol-gel synthesis have been reported by Riaz et al. 2014a and Akbar et al. 2014a. pH of sol is varied as 1, 2, 3 and 4. Films were deposited on glass substrates. Before use, these substrates were cleaned with acetone and isopropyl alcohol in ultrasonic bath for 15 minutes, separately.

Thin films were characterized structurally using Bruker D8 Advance X-ray Diffractometer with $\text{CuK}\alpha$ radiations ($\lambda=1.5406\text{\AA}$). For studying optical properties J.A. Woollam's M-2000 Variable Angle Spectroscopic Ellipsometer was used.

3. RESULTS AND DISCUSSION

XRD patterns for iron oxide films can be seen in Fig. 1. Existence of peaks matching to planes (012), (104), (110), (202), (024) and (217) point toward hematite ($\alpha\text{-Fe}_2\text{O}_3$) phase. No peaks corresponding to other oxide were observed. With increase in pH to 4 the crystallinity of iron oxide thin films increases.

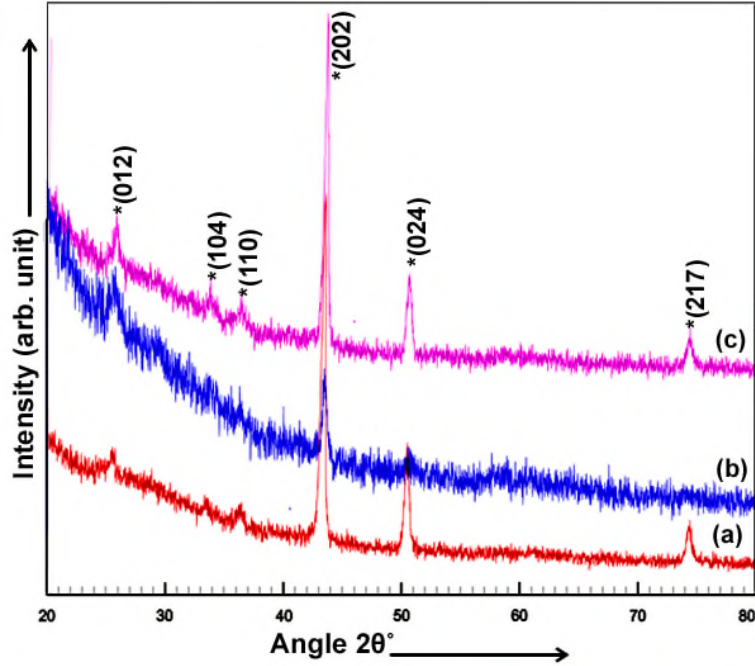


Fig. XRD patterns for iron oxide thin films with pH (a) 2 (b) 3 (c) 4 (* α -Fe₂O₃)

Crystallite size (t) (Cullity 1956), dislocation density (δ) (Kumar et al. 2011) and lattice parameters (Cullity 1956) were calculated using Eqs. 1-3

$$t = \frac{0.9\lambda}{B \cos \theta} \quad (1)$$

$$\delta = \frac{1}{t^2} \quad (2)$$

$$\sin^2 \theta = \frac{\lambda^2}{3a^2} (h^2 + k^2 + hk) + \frac{\lambda^2 l^2}{4c^2} \quad (3)$$

Where, θ is the diffraction angle, λ is the wavelength (1.5406Å) and B is Full Width at Half Maximum. Crystallite size increases as pH was increased from 1 to 5 leading to decrease in dislocation density. As pH of the films increases, number of hydroxyl ions increases that leads to high condensation reaction. Thus repulsive forces between the grains decreases that lead to increase in crystallite size (Riaz and Naseem 2015). Lattice parameters are close to that reported in literature. It can be seen that x-ray density increases as pH of sol was increased.

Table 1 Structural parameters for iron oxide thin films

pH	Crystallite size (nm)	Dislocation density (10^{15} lines/m ²)	Lattice parameters (Å)		Unit cell volume (Å ³)	X-ray density (g/cm ³)
			A	c		
1	22.50	1.975309	5.016	13.605	296.4364	5.433231
2	23.42	1.823166	5.008	13.600	295.383	5.452608
3	23.98	1.739008	4.998	13.586	293.9016	5.48009
4	24.78	1.628536	4.902	13.532	281.596	5.719568

Iron oxide thin films showed high transmission as shown in Fig 2. The sharp increase in transmission at ~500nm was an indicative of direct transition in iron oxide. It can be seen that transmission of the films increase as pH was increased to 4. This increase in transmission is associated with increase in crystallite size (Table 1). Increase in grain size leads to decrease in grain boundaries that act as scattering center for incident photons (Riaz and Naseem 2015). This thus leads to increase in transmission. Tauc method was used for determination of band gap of the films (Fig. 3). The values of band gap (2.18-2.210eV) are close to that reported in literature.

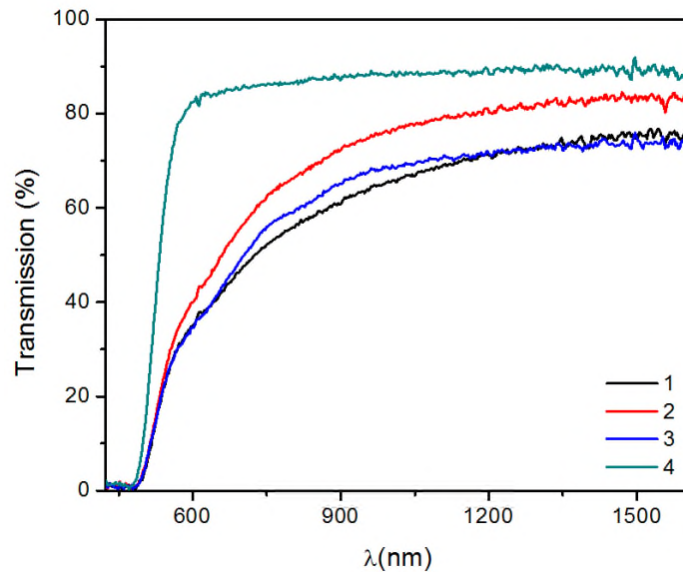


Fig. 2 Transmission curves for iron oxide thin films

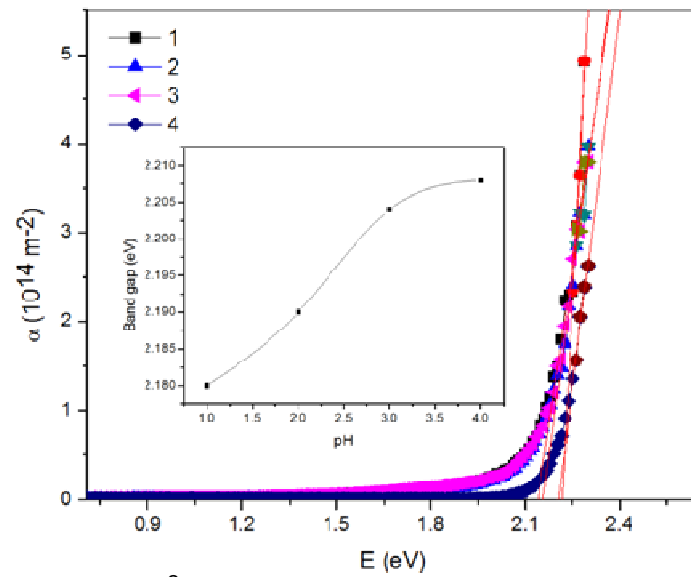


Fig. 3 α^2 vs. E (eV) for iron oxide thin films

Optical parameters of iron oxide thin films were then studied using M-2000 Variable Angle Spectroscopic Ellipsometer. It is non-destructive, high precision and fast measurement technique. There were two common limitations on the ellipsometry measurements; 1) Roughness of the films and 2) Angle of measurement (Riaz and Naseem 2015). So here incidence angle was chosen close to Brewster angle. The sensitivity of these measurements are maximized at Brewster angle. For obtaining low MSE (mean square error), fitting parameters were varied (Riaz and Naseem 2015). The surface roughness was approximated through Bruggeman effective medium approximation (EMA) where a mixture of 50% voids/air and 50% sample material was used. Figure 4 shows that model used in the study gives the best fit between the experimental and fitted data.

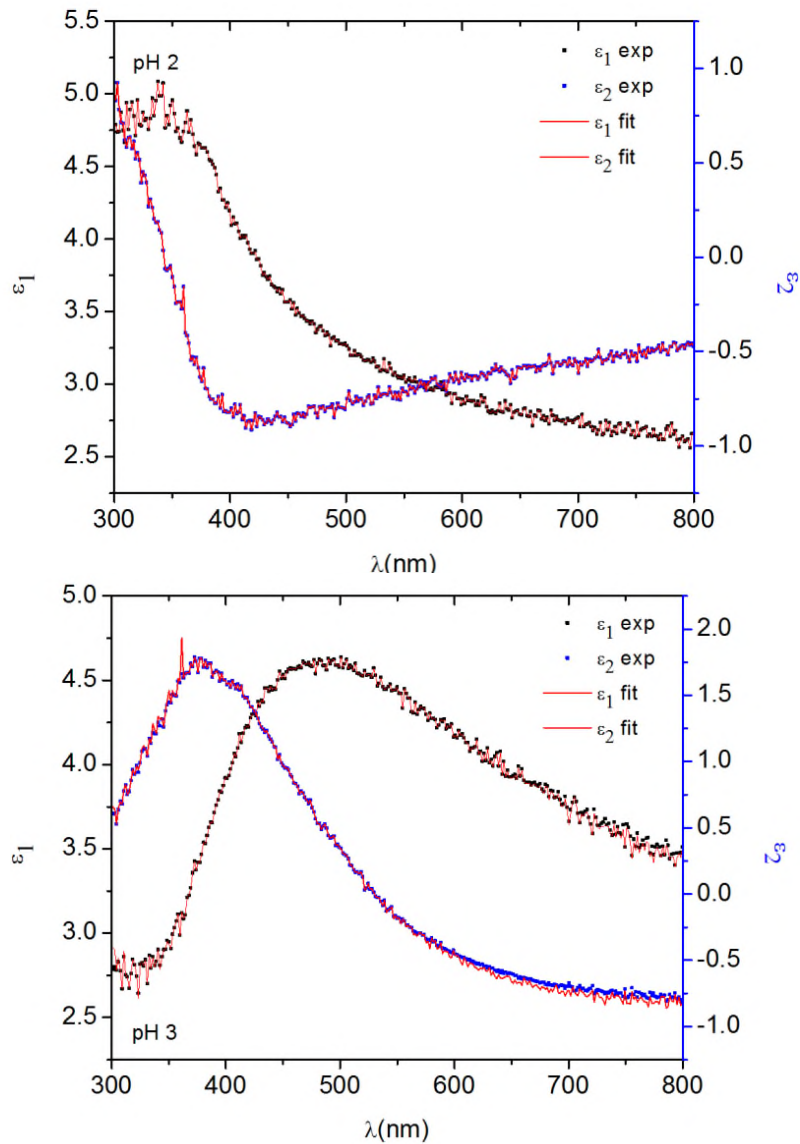


Fig. 4 Model fitting for iron oxide thin films

Refractive index and extinction coefficient (Fig. 5) was found to be decreased and became constant at high wavelength showing normal dispersion behavior. High refractive index of iron oxide thin films made them a suitable candidate for solar cell application. It can be seen that in larger wavelength region the highest refractive index and lowest extinction coefficient was observed for films with pH 4. This increase in refractive index is associated with increase in density of the films (Riaz and Naseem 2015) as was observed in table 1.

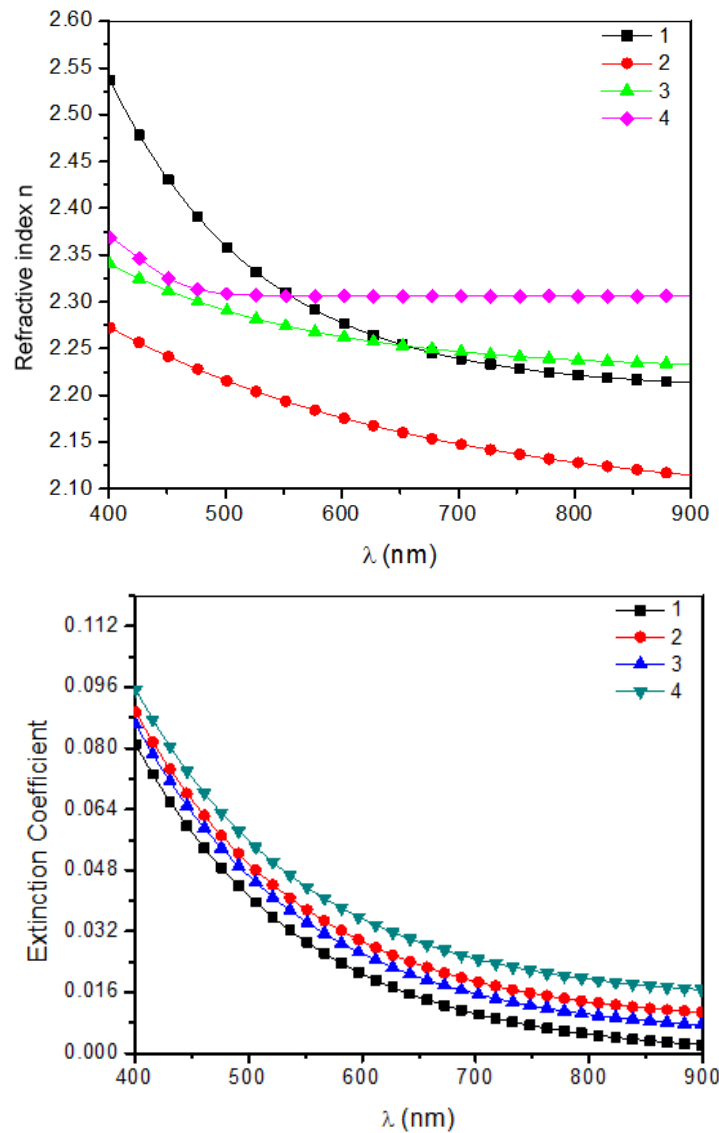


Fig. 5 Refractive index and extinction coefficient for iron oxide thin films

4. CONCLUSIONS

In this research work, pH of iron oxide sols was used as 1, 2, 3 and 4. Bruker D8 advance X-ray diffractometer was used to study the structural properties. J.A Woollams Variable Angle Spectroscopic Ellipsometer was used for optical properties determination. X-ray diffraction results indicate hematite phase of iron oxide. Crystallinity and crystallite size increases with increase in pH. Due to high crystallite size, scattering from grain boundaries decreases thus, resulting in increase in transmission with pH. Band gap of iron oxide films is in the range of 2.18-2.210eV. Increase in refractive index and decrease in extinction coefficient is associated with increase in x-ray density of iron oxide thin films.

REFERENCES

- Akbar, A., Riaz, S., Ashraf, R. and Naseem, S. (2014a), "Magnetic and magnetization properties of Co-doped Fe₂O₃ thin films," *IEEE Trans. Magn.*, **50**, 2201204
- Akbar, A., Riaz, S., Bashir, M. and Naseem, S. (2014b), "Effect of Fe³⁺/Fe²⁺ ratio on superparamagnetic behavior of spin coated iron oxide thin films," *IEEE Trans. Magn.*, **50**, 2200804
- Akbar, A., Riaz, S., Ashraf, R. and Naseem, S. (2015), "Magnetic and magnetization properties of iron oxide thin films by microwave assisted sol-gel route," *J. Sol-Gel Sci. Technol.*, **74**, 320–328.
- Ali, M.A., Khan, MN.I., Chowdhury, F.U.Z., Akhter, S., Uddin, M.M. (2015), "Structural Properties, Impedance Spectroscopy and Dielectric Spin Relaxation of Ni-Zn Ferrite Synthesized by Double Sintering Technique," *J. Sci. Res.*, **7**, 65-75.
- Aragon, F.F.H., Ardisson, J.D., Aquinoa, J.C.R., Gonzalez, I., Macedo, W.A.A., Coaquira, J.A.H., Mantilla, J., Silva, S.W. and Morais, P.C. (2016), "Effect of the thickness reduction on the structural, surface and magnetic properties of α-Fe₂O₃ thin films," *Thin Solid Films*, **607**, 50–54.
- Craik, D.J. (1975), *Magnetic Oxides*, John Wiley & Sons, New York.
- Cullity, B.D. (1956), "Elements of x-ray diffraction," Addison Wesley Publishing Company, USA.
- Kulkarni, S.S. and Lokhande, C.D. (2003), "Structural, optical, electrical and dielectrical properties of electrosynthesized nanocrystalline iron oxide thin films," *Mater. Chem. Phys.*, **82**, 151–156.
- Kumar, N., Sharma, V., Parihar, U., Sachdeva, R., Padha, N. and Panchal, C.J. (2011) "Structure, optical and electrical characterization of tin selenide thin films deposited at room temperature using thermal evaporation method," *J. Nano- Electron. Phys.*, **3**, 117-126
- Riaz, S. and Naseem, S. (2015), "Controlled nanostructuring of TiO₂ nanoparticles: a sol-gel approach," *J. Sol-Gel Sci. Technol.*, **74**, 299–309
- Riaz, S., Akbar, A. and Naseem, S. (2014a), "Ferromagnetic Effects in Cr-Doped Fe₂O₃ Thin Films," *IEEE Trans. Magn.*, **50**, 2200704
- Riaz, S., Ashraf, R., Akbar, A. and Naseem, S. (2014b), "Microwave Assisted Iron Oxide Nanoparticles—Structural and Magnetic Properties," *IEEE Trans. Magn.*, **50**, 2201504
- Vanags, M., Sutka, A., Kleperis, J. and Shipkovs, P. (2015), "Comparison of the electrochemical properties of hematite thin films prepared by spray pyrolysis and electrodeposition," *Ceram. Int.*, **41**, 9024–9029.